This article was downloaded by: [Tomsk State University of Control Systems and Radio]
On: 23 February 2013, At: 03:19
Publisher: Taylor & Francis
Informa Ltd Registered in England and Wales Registered Number: 1072954
Registered office: Mortimer House, 37-41 Mortimer Street, London W1T 3JH, UK

Molecular Crystals and Liquid Crystals
Publication details, including instructions for authors and subscription information:
http://www.tandfonline.com/loi/gmcl16

Transport, Magnetic and Structural Studies of Polyacetylene

A. J. Heeger [a] & A. G. Maciarmid [a]
[a] Laboratory for Research on the Structure of Matter, University of Pennsylvania, Philadelphia, Penna
Version of record first published: 19 Dec 2006.

To cite this article: A. J. Heeger & A. G. Maciarmid (1981): Transport, Magnetic and Structural Studies of Polyacetylene, Molecular Crystals and Liquid Crystals, 77:1-4, 1-24

To link to this article: http://dx.doi.org/10.1080/00268948108075226

PLEASE SCROLL DOWN FOR ARTICLE

Full terms and conditions of use: http://www.tandfonline.com/page/terms-and-conditions

This article may be used for research, teaching, and private study purposes. Any substantial or systematic reproduction, redistribution, reselling, loan, sub-licensing, systematic supply, or distribution in any form to anyone is expressly forbidden.

The publisher does not give any warranty express or implied or make any representation that the contents will be complete or accurate or up to date. The accuracy of any instructions, formulae, and drug doses should be independently verified with primary sources. The publisher shall not be liable for any loss, actions, claims, proceedings, demand, or costs or damages

whatsoever or howsoever caused arising directly or indirectly in connection with or arising out of the use of this material.

Downloaded by [Tomsk State University of Control Systems and Radio] at 03:19 23 February 2013

Mol. Cryst. Liq. Cryst., 1981, Vol. 77, pp. 1–24
0026-8941/81/7701-0001$06.50/0
© 1981 Gordon and Breach, Science Publishers, Inc.
Printed in the United States of America

(Proceedings of the International Conference on Low-Dimensional Conductors, Boulder, Colorado, August 1981)

Downloaded by [Tomsk State University of Control Systems and Radio] at 03:19 23 February 2013

TRANSPORT, MAGNETIC AND STRUCTURAL STUDIES OF POLYACETYLENE

A.J. HEEGER, A.G. MACDIARMID
Laboratory for Research on the Structure of Matter
University of Pennsylvania
Philadelphia, Penna.

Received for publication September 14, 1981

Experimental progress is reviewed with emphasis on magnetic and transport studies. The magnetic results are fully consistent with the soliton doping mechanism; the decrease in Curie-law contribution has been demonstrated; the Pauli term remains small ($Y < 0.07$) and is apparently zero in the limit of completely uniform doping. The electrical conductivity (P and T dependence) and thermopower (n-type and p-type) are in excellent agreement with Kivelson's theory of intersoliton electron hopping.

I. INTRODUCTION

A decade has passed since the initial work on NMP-TCNQ focussed interest on the study of organic one-dimensional conductors. There has been remarkable progress. The Peierls instability, commensurate and incommensurate change density wave (CDW) states, and collective mode CDW transport have been established experimentally.[1] More recently, the $(TMTSF)_2X$ systems have been shown to exhibit a spin-density-wave ground state[2] in close competition with superconductivity.[3] The class of organic metals has been greatly expanded through the creativity of synthetic organic chemistry, while simultaneously entirely new physical concepts have emerged from a wealth of experimental data. It is indeed gratifying to see that in only a few years, 1-d organic conductors have progressed from delic-

ate, tiny molecular crystals with a single-crystal electrical conductivity of less than $10^2(\Omega\text{-cm})^{-1}$ to bona fide metals which exhibit superconductivity at low temperatures.

Although initial work in this general area focused on delicate molecular crystals, it was clear from the beginning that a longer term goal was to expand the field into potentially useful polymer systems. Recent progress on chemically doped polyacetylene, $(CH)_x$, and related conjugated polymers has opened a new class of organic conductors with electrical properties that can be systematically varied through chemical and/or electrochemical doping to span the full range from insulator to semiconductor to metal. The existing experimental data show that these materials have potential for use in a number of areas of future technology. Experimental studies at the University of Pennsylvania have demonstrated that doped polyacetylene might be useful in such diverse applications as: (1) the replacement of increasingly scarce conventional conductors by synthetic metals; (2) the development of light-weight, high-energy-density batteries; and (3) low-cost solar photovoltaic materials. The electrical conductivity of polyacetylene can be varied in a controlled manner over thirteen orders of magnitude through chemical or electrochemical doping. Values greater than $3 \times 10^3\ \Omega^{-1}\text{cm}^{-1}$ have already been achieved with only partially crystalline samples, and analysis of the transport[4] and optical[5] data implies that a further increase of at least one order of magnitude should be possible. Controlled electrochemical doping and "undoping" have been demonstrated,[6] and prototype high-energy-density rechargeable batteries have been constructed using $(CH)_x$ as both the active cathode and anode.[7] Photovoltaic phenomena have been observed in heterojunctions,[8] Schottky-barrier junctions[9] and photo-chemical junctions.[10] Thus, although these and other potential applications will require considerable future work before technological value can be determined, the properties appear promising.

Polyacetylene is the simplest conjugated polymer. It consists of weakly coupled chains of CH units forming a quasi-one-dimensional lattice. Three of the four carbon valence electrons are in sp^2 hybridized orbitals; two of the σ-type bonds construct the 1-d lattice while the third forms a bond with the hydrogen side group. The 120° bond angle between these three bonds can be satisfied by two possible arrangements of the carbon atoms, trans - $(CH)_x$ and cis - $(CH)_x$, as shown in Fig. 1.

Downloaded by [Tomsk State University of Control Systems and Radio] at 03:19 23 February 2013

Downloaded by [Tomsk State University of Control Systems and Radio] at 03:19 23 February 2013

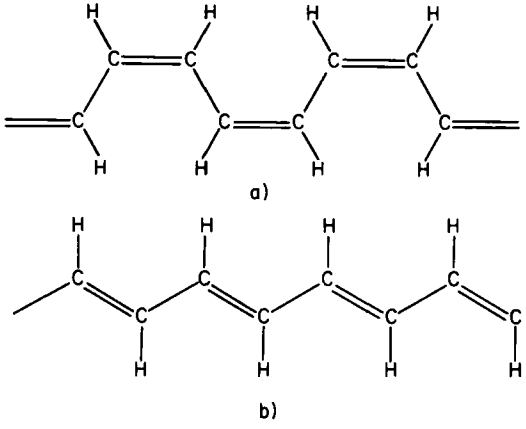

FIGURE 1. Structural formulas:(a) cis-$(CH)_x$; (b) trans-$(CH)_x$.

Simple estimates lead to a picture of $(CH)_x$ as a broad-band, quasi-one-dimensional semiconductor. The overall bandwidth associated with electronic motion along the chain, $W_{\|} = 2z\beta$, where z is the number of nearest neighbors and β is the intercarbon transfer integral for π-electrons. From theoretical and spectroscopic studies of aromatic ring systems and short-chain polyenes, β can be estimated as 2.5 - 3.0 eV so that $W_{\|} \sim$ 10-12 eV. The carriers generated by the doping of $\|(CH)_x$ result from charge transfer. Charge transfer occurs from polymer to acceptor (A) with the polymer chain acting as a poly(cation) in the presence of an A^- species. For a donor(D), the polymer chain acts as a poly(anion) in the presence of D^+ species. The A^- or D^+ ions reside between polymer chains. Reversible doping can be carried out electrochemically, and chemical compensation has been demonstrated. For example, after doping and subsequent chemical compensation, the optical absorption spectrum converts back to that of the undoped polymer.[11] Therefore, since the anisotropic optical properties of the undoped polymer are characteristic of the quasi-one-dimensional $(CH)_x$ chains, the reversibility implies that the $(CH)_x$ chains remain intact in the doped polymer.

II. SOLITONS (WITHOUT MATHEMATICS!) IN POLYACETYLENE

The mathematical theory[12-15] of solitons in $(CH)_x$ has been investigated in detail in several recent papers which show that the coupling of these conformational excitations to the π-electrons leads to unusual electrical and magnetic properties. The possibility of experimental studies of such solitons in polyacetylene, therefore, not only promises a deeper understanding of this important conducting polymer, but also represents a unique opportunity to explore nonlinear phenomena in condensed matter. In the following paragraphs we describe the concepts and theoretical results in simple, schematic terms. Where necessary we refer to specific theoretical results; however, the fundamental origins of these novel concepts can be at least qualitatively understood in elementary terms.

If the bond lengths in pure trans-$(CH)_x$ were uniform, the polymer would be a quasi-one-dimensional metal with a half-filled band. Such a system is unstable with respect to a dimerization distortion (the Peierls instability) in which adjacent CH groups move towards each other, forming alternately short (or double) bonds and long (or single) bonds, thereby lowering the energy of the system and opening the semiconductor band gap.[1]

The existence of bond alternation in trans-$(CH)_x$ is fundamental to the soliton concept. Only recently, however, has direct experimental evidence of the dimerization distortion been obtained from X-ray scattering studies by Fincher et al.[16] They find a crystal structure similar to that proposed earlier by Baughman[17] (space group $P2_1/n$ with a = 4.25Å, b = 7.33Å, c = 2.46Å, β = 91.4°, and two chains per unit cell). The structure is dimerized as shown schematically in Figure 2 with u_o = 0.03 ± 0.01Å.

This value for the dimerization distortion will result in an energy gap in the electronic excitation spectrum. Using the SSH Hamiltonian, the one-dimensional energy gap (E_g^{1d}), appropriate for $\vec{k}$ parallel to the chain axis in reciprocal space, can be written as

$$E_g^{1d} \equiv 2\Delta = 8\beta u_o \qquad (1)$$

where β is the electron-phonon coupling constant. Analysis of the optical absorption data leads to a value for $E_g^{1d} \simeq$ 1.6-1.8 eV. This value, when substituted into eq. 1 leads to an estimate for the electron-photon coupling; $4 < \beta < 8$eV/Å, in agreement with estimates obtained from studies of lattice

Downloaded by [Tomsk State University of Control Systems and Radio] at 03:19 23 February 2013

dynamics in polyacetylene.[12,18] Thus the existence of bond alternation in long chain polyenes has been confirmed. Moreover, the good agreement between the measured energy gap and that predicted by the SSH electron-lattice Hamiltonian (using the measured distortion) implies that the effective electron-electron interaction is relatively weak and does not dominate the physics.

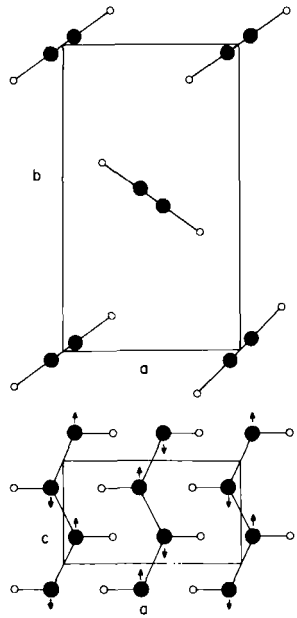

Figure 2. Schematic view of trans-$(CH)_x$ structure projected onto the a-c plane (open circles indicate H, closed circles indicate c). The dimerization distortion (U_o) is indicated. Note that the central chain is displaced along b by one-half the unit cell (see Fincher et al, ref.).

Clearly, by symmetry, one could interchange the double and single bonds in trans-$(CH)_x$ without changing the energy. Thus, there are two degenerate lowest-energy states, A and B, having two distinct bonding structures as shown in Figure 3. This twofold degeneracy leads to the existence of nonlinear

Downloaded by [Tomsk State University of Control Systems and Radio] at 03:19 23 February 2013

topological excitations, bond-alternation domain walls or solitons, which appear to be responsible for many of the remarkable properties of $(CH)_x$.

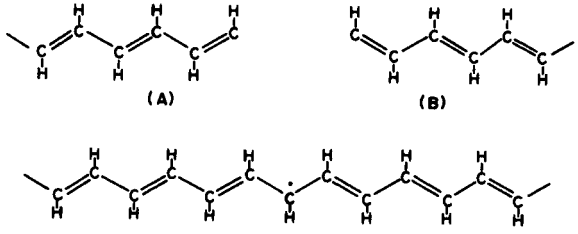

Figure 3. Formation of a neutral soliton by joining together the two lowest energy states, (A) and (B) of trans-$(CH)_x$.

Associated with the kink is an electronic bound state with energy at mid-gap; i.e., halfway between the bonding valence band and the antibonding conduction band (Fig. 4). If the localized state contains one electron, the soliton is neutral, with spin 1/2, and therefore is paramagnetic. When the electron in the localized state is removed, for example by acceptor doping, the soliton is positively charged, with spin zero and nonmagnetic.

Downloaded by [Tomsk State University of Control Systems and Radio] at 03:19 23 February 2013

Downloaded by [Tomsk State University of Control Systems and Radio] at 03:19 23 February 2013

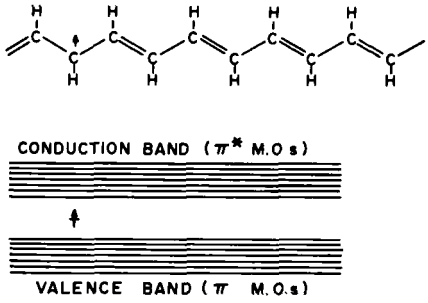

Figure 4. Diagrammatic representation of a neutral soliton (free radical located on a non-bonding π molecular orbital) in trans-$(CH)_x$.

The positive soliton (Fig. 5) is equivalent to a stabilized (by delocalization) carbonium ion on the $(CH)_x$ chain. Similarly, double occupancy induced by donor doping would lead to a spin-zero negatively charged state. The negative soliton is thus equivalent to a stabilized carbanion as shown in Figure 6.

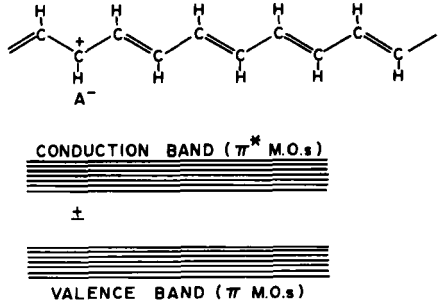

FIGURE 5. Diagrammatic representation of a positive soliton (carbonium ion located on a non-bonding π molecular orbital) in trans-$(CH)_x$.

Downloaded by [Tomsk State University of Control Systems and Radio] at 03:19 23 February 2013

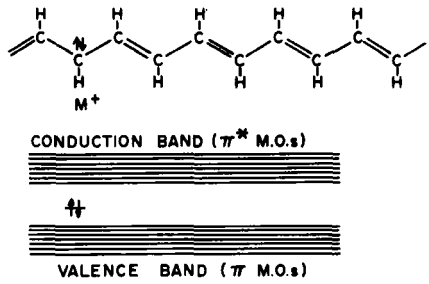

Figure 6. Diagrammatic representation of a negative soliton (carbanion located on a non-bonding π molecular orbital) in trans-$(CH)_x$.

When a single chain of cis-$(CH)_x$ begins to isomerize, the isomerization process can, in principle, commence at different parts of the chain, one having configuration (A), the other, configuration (B). When these two different configurations meet, a free radical is produced as shown schematically in Figure 3. This has been confirmed experimentally - when pure cis-$(CH)_x$, possessing no free spins, undergoes isomerization, approximately one in 3000 of the (CH) units in the resulting trans-$(CH)_x$ is in the form shown in Figure 3 with an unpaired spin and a Curie law magnetic susceptibility. This species is actually a valid excited state of trans-$(CH)_x$, which could be formed in principal, for example, if trans-$(CH)_x$ could be heated to a sufficiently high temperature without thermal decomposition. It would be expected that this free spin could be readily ionized leaving behind a positive

charge. This has indeed been observed. Thus if $(CH)_x$ is carefully and slowly oxidized by, for example, AsF_5, a stabilized carbonium ion is formed; the Curie spins originally present decrease almost to zero, and the conductivity of the material increases greatly.[19]

The presence of neutral solitons induced as defects during isomerization is a fortunate accident, for the number of thermally induced neutral soliton excitations in undoped $(CH)_x$ would be far too small to be observable. In this context, however, it must be stressed that it is not necessary to first have neutral solitons in order to obtain positive (or negative) solitons. Since the nonbonded localized state appears at the center of the energy gap, i.e., the chemical potential, the relevance of the solitons to the doping of $(CH)_x$ depends on the energy for creation of a soliton, E_s, as compared with the energy required for making an electron or a hole, $E_g \equiv 2\Delta$

If $\Delta < E_s$, charge-transfer doping would occur by creating free band excitations; if $\Delta > E_s$, soliton formation would be favored. Both numerical calculations[12] using a discrete lattice model and analytical results for a continuum model[14] indicate that, within the one-electron approximation, $\Delta > E_s$ (the continuum model yields $E_s = 2\Delta/\pi$). Thus, for example, oxidation by a nearby acceptor leads to a charged, nonmagnetic kink (Figure 6). This has been confirmed experimentally. For example, on careful p-doping of $(CH)_x$ with AsF_5 one finds that: (i) the original free Curie spins in $(CH)_x$ decrease as indicated above and (ii) even though the amount of dopant species is far in excess of that necessary to remove the original free spins, no additional Curie spins appear.[20]

For simplicity, the solitons are shown in Figures 3-6 as if localized on one lattice site, whereas detailed calculations[12] have shown that minimization of the energy spreads the kink over a region of about 15 (CH) units. Thus in the case of a positive soliton, although the maximum charge density is adjacent to the counter anion, A^-, ~85% of the charge is spread out symmetrically on either side over ~15 (CH) units. This is qualitatively understandable, since it is recognized from symmetry considerations that the positive soliton formally located on a single (CH) unit will actually have some interaction with the p_π orbitals on the adjacent (CH) units. This delocalizes the non-bonding mid-gap state over many bond-lengths as shown schematically in Figure 7. It is apparent that considerable bond length distortion will be involved near the center of the soliton, since these bonds alone are responsible for adjusting the bond lengths of segment (A) with those of segment (B) Figure 7(a) in which the relative positions of the formally single and double bonds are reversed.

Downloaded by [Tomsk State University of Control Systems and Radio] at 03:19 23 February 2013

Since the energy to distort a bond is proportional to the square of the distortion, it is apparent that if the distortion

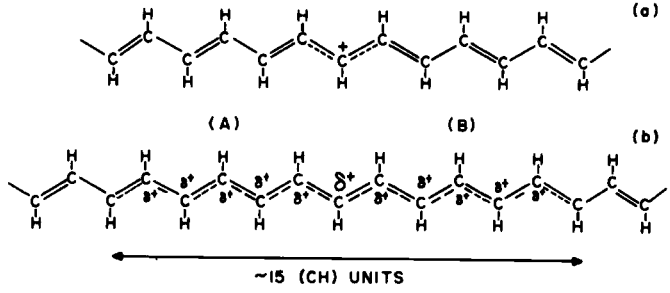

Figure 7. Diagrammatic representation of the delocalization of a positive soliton in trans-$(CH)_x$: (a) charge localized on one (CH) unit; (b) charge localized over ~15 (CH) units.

were spread out over several bonds, the distortional energy required would be less. Hence, the system is stabilized if the bond distortion is taken up by several bonds as shown diagrammatically in Figure 7(b) to produce a positive soliton or domain wall, which separates (A) type domains from (B) type domains. We note that within these domain walls (particularly near the center), the C-C bond lengths tend to become very nearly equal. It might at first be thought that the greatest stabilization would result if the distortion were spread out over the whold chain. This, however, is not the case because of the Peierls distortion stabilizing energy, which, for a hypothetical 1-dimensional molecule, predicts that a single-

Downloaded by [Tomsk State University of Control Systems and Radio] at 03:19 23 February 2013

double bond alternating structure has a lower total energy and thus, is more stable than one consisting totally of equal (bond order 1.5) linkages. These two opposing distortional effects involving bond lengths result in the soliton domain walls in $(CH)_x$ being extended to approximately 15(CH) units.

III. SOLITONS IN POLYACETYLENE: EXPERIMENTAL CONSEQUENCES

Recent experimental results on the magnetic properties, lattice dynamics, energy level structure, electrical transport, and photoexcitations are in agreement with the soliton model. The data indicate that injection of an electron-electron (hole-hole) pair by chemical doping or photoinjection of an electron-hole pair invariably distort the lattice leading to formation of a soliton-antisoliton pair. These results indicate that unlike traditional semiconductors, the polyacetylene lattice is inherently unstable in the presence of electron and/or hole excitations. The data on the lattice dynamics[18] (soliton induced infra-red active vibrational modes), the spectroscopy of the mid-gap state,[21] and photoexcitations[22] (luminescence and photoconductivity) are reviewed by Etemad et al[23] in these proceedings. In this section, we focus on the magnetic and transport properties.

Magnetic Properties

Charged solitons are spinless. Thus if doping occurs via the generation of charged solitons, the charge carriers would be spinless, and the localized states generated by dilute doping would not show paramagnetism. Our earlier results[19] for the magnetic susceptibility of lightly doped samples were consistent with the soliton doping concept. The Curie-law contribution decreased, while the Pauli term (χ_p) remained small and was apparently zero in the limit of completely uniform doping.

The magnetic susceptibility results, however, have been controversial. Tomkiewicz et al[24] presented data [primarily from doped cis-$(CH)_x$] which suggested a linear increase in χ_p with doping, in contrast to the abrupt step-like increase found by Ikehata et al.[19]

In an attempt to resolve these questions, a collaborative experiment between the Penn and IBM groups was carried out. Polyacetylene film was prepared independently by the two groups. Isomerization and doping were subsequently carried out jointly by T.C. Clarke (IBM) and M. Druy and T. Woerner (Penn) using the techniques described earlier. Samples

Downloaded by [Tomsk State University of Control Systems and Radio] at 03:19 23 February 2013

Downloaded by [Tomsk State University of Control Systems and Radio] at 03:19 23 February 2013

of $[CH(AsF_5)_y]_x$ were prepared in the important transitional region, $Y \simeq 0.03$. Susceptibility measurements utilized both the Schumacher-Slichter technique (using 10 MHZ radiation) and a standard 10GHz epr spectrometer. In the former technique the sample contains its own standard in the form of the known absolute susceptibility (χ_N) of the protons (and/or ^{19}F nuclei) in the sample. Moreover, the low frequency (10MHz) avoids any possible complications from skin effect and non-uniform rf fields in the highly conducting samples ($\sigma \simeq 50\text{-}100\ \Omega^{-1}\text{-cm}^{-1}$) since both the standard (χ_N) and the unknown susceptibility (χ_p) resonances come from precisely identical regions of the sample. The 10GHz ESR measurement utilizes an external standard.

Consistent with the high measured dc conductivities (see Table 1), the 10GHz ESR lines showed the familiar asymmetric Dyson line shape. The low frequency Schumacher-Slichter experiment avoided these skin-depth complications altogether resulting in symmetric lineshapes. The Schumacher-Slichter results (S. Ikehata) for the spin susceptibility at 77K for the three samples at intermediate doping and a metallic control sample (Y = 0.12) are given in Table 1. The results are consistent with the earlier data of Ikehata et al which indicated a low susceptibility for $Y < 0.07$ with a step-like increase to Typical metallic values above $Y = 0.07$.

The raw data (77K) for Y = 0.12 and Y = 0.036 are compared dircectly on Figure 8. Examination of the figure clearly demonstrates that the susceptibility of the 3.6% sample is approximately 1/30 of the 12% sample. More precise values were obtained by direct integration. The ESR signal from the Y = 0.036 sample (77K) is shown more clearly in Fig. 9 (the increased signal-to-noise was obtained by increasing the magnitude of the modulation field and by using a much longer time constant). The ESR lines are narrow ($0.85 < \Delta H_{pp} < 1.1$ gauss) and symmetric.

Direct integration of the 10GHz Dysonian ESR lines yield

TABLE 1 Schumacher - Slichter Results for the Spin Susceptibility (χ_p) for $[CH(AsF_5)_y]_x$ (IBM-Penn Joint Experiment)

Y	$\sigma(\Omega^{-1}\text{-cm}^{-1})$	χ_p(emu/mole)
0.12	250	3.3×10^{-6}
0.036	60	1.5×10^{-7}
0.032	110	1.2×10^{-7}
0.023	40	1.0×10^{-7}

TABLE 2 10GHz ESR Results for $[CH(AsF_5)_y]_x$ (IBM-PENN Joint Experiment)

Y	Skin-depth (microns)	Sample thickness (microns)	χ_p (emu/mole)	χ_p (corrected) [see text]
0.036	65	60-80	6.5×10^{-7}	$\sim 2.2 \times 10^{-7}$
0.032	50	150	3.1×10^{-7}	$\sim 1.0 \times 10^{-7}$
0.023	80	60-80	3.9×10^{-7}	$\sim 1.3 \times 10^{-7}$

somewhat larger values for χ_p as indicated in Table 2. The 10GHz results obtained at PENN (J. Flood) and at IBM (Y. Tomkiewicz) were in agreement within experimental error.,

The various potential problems with the 10GHz measurements result from the high conductivity and the associated assymmetric lineshape. Note, however, that at least for the Y = 0.036 and Y = 0.032 samples the skin depth is comparable to the sample thickness. Thus, since the microwave fields penetrate from both sides essentially the entire volume of the sample contributes. However, the highly conducting samples lead to lineshape distortions which complicate the analysis. This is shown clearly in Fig. 10 where we show the raw data and first integral of the ESR from the Y = 0.12 sample (σ = 250 Ω^{-1}-cm^{-1}). The lineshape is clearly Dysonian. Note the extreme breadth of the line (long tail on high field side of the 1^{st} integral). Although the signal returns eventually to the baseline, the area under the curve (i.e. the apparent susceptibility) is at least about a factor of three too large because of the distorted lineshape. In fact, direct integration of the data yields a value for χ_p = 8×10^{-6} emu/mole whereas the correct value (from static Faraday balance measurements[20,25] and from Schumacher-Slichter measurements) for heavily doped metallic $(CH)_x$ is $\chi_p = 3 \times 10^{-6}$ emu/mole. Similar effects are seen in the intermediate range samples. Note (Table 1) that the conductivities of all four samples are comparable (σ = 50-100 Ω^{-1}-cm^{-1} for the Y = 2-4% and σ = 250 Ω^{-1}-cm^{-1} for Y = 12%). Again (see Fig. 11) the Dyson lineshape leads to a distorted 1^{st} integral with a long tail on the high field side and an area apparently much greater than that of the pure absorption.

This distorted lineshape and long high field tail are clearly a problem. The direct integration of the 10GHz Dyson lineshape, therefore, does not reproduce the correct absorption curve. Thus, the second integral (i.e. the susceptibility) cannot be trusted. The distorted shape and excessive

Downloaded by [Tomsk State University of Control Systems and Radio] at 03:19 23 February 2013

Downloaded by [Tomsk State University of Control Systems and Radio] at 03:19 23 February 2013

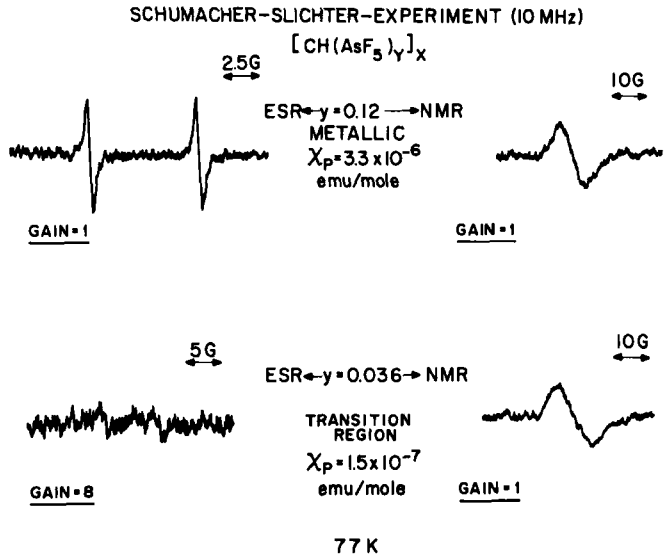

FIGURE 8. Recorder tracings from Schumacher-Slichter experiment comparing the Y = 0.12 and the Y = 0.036 samples.

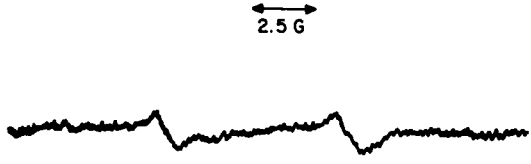

FIGURE 9. Low field ESR from Y = 0.036 sample (see Fig. 8) showing the lineshape and linewidth more clearly.

Downloaded by [Tomsk State University of Control Systems and Radio] at 03:19 23 February 2013

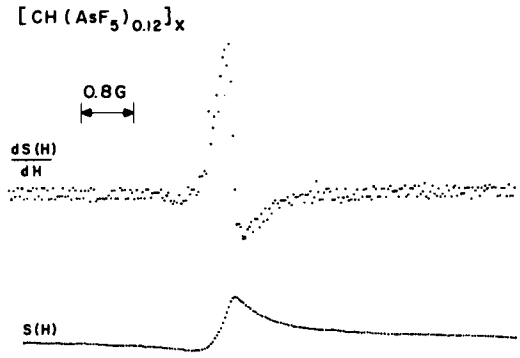

FIGURE 10. Derivative signal and first integral for metallic sample, Y = 0.12.

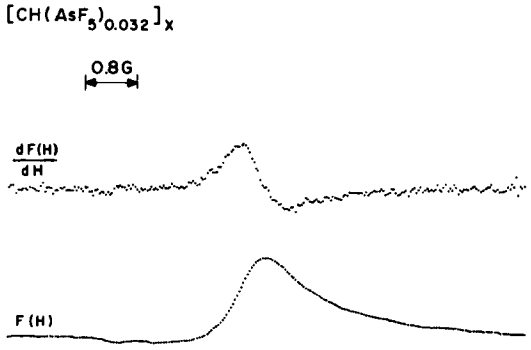

FIGURE 11. Derivative signal and first integral for Y = 0.032.

high field tail overestimate the true area of the absorption curve by about a factor of three. If one attempts to correct for the distorted lineshape and reduces the apparent χ_p obtained from the 10GHz experiments by this factor, the resulting values are essentially in agreement (see Tables 1 and 2) with those obtained by the Schumacher-Slichter method. Moreover, the Schumacher-Slichter results stand on their own: the sample contains its own internal standard; the lineshape is symmetric; the same technique was used for all four samples with σ increasing only modestly from 50-100 Ω^{-1}-cm^{-1} in the 2-4% range to 250 Ω^{-1}-cm^{-1} at 12%; the low susceptibility results were even independently cross-checked by using both ^{1}H and ^{19}F nuclei.

Our conclusions regarding the magnetic spin susceptibility are as follows:

i) It is possible to prepare highly conducting samples ($\sigma \sim 100\ \Omega^{-1}$-cm^{-1}) for Y ~ 3-4% with $\chi_p \simeq 1 \times 10^{-7}$ emu/mole.

ii) There is a major increase in χ_p near Y $\simeq$ 7% where χ_p increases from a value $\leq 1 \times 10^{-7}$ to $\chi_p \simeq 3.3 \times 10^{-6}$ emu/mole in the "metallic" limit.

iii) Higher values of χ_p can be obtained (and have been demonstrated) in the intermediate doping range (i.e. Y ~ 2-5%) by rapid doping. The step-like increase near Y = 7% makes the measured values extremely sensitive to the uniformity of doping. Hence any small residual χ_p in the intermediate regime (Y < 7%) may be the result of residual non-uniformity in doping through the sample.

The magnetic susceptibility results for AsF_5 doped trans-$(CH)_x$ are, therefore, fully consistent with the soliton doping mechanism. The decrease in the Curie-law contribution has been demonstrated; the Pauli term, χ_p, remains small (for Y < 0.07) and is apparently zero in the limit of completely uniform doping.

Electrical Transport (D. Moses, J. Chen, A. Denenstein, M. Kaveh, T.-C. Chung, A.J.Heeger and A.G. MacDiarmid, Sol. St. Commun, in press)

The development of a basis for understanding electrical transport within the soliton theory remains as an interesting and important problem. Kivelson[26] has recently proposed a novel transport mechanism appropriate to the regime of dilute doping. He suggested that in lightly doped trans-$(CH)_x$, phonon assisted electron-hopping between soliton mid-gap bound states

Downloaded by [Tomsk State University of Control Systems and Radio] at 03:19 23 February 2013

could be the dominant mechanism. The resulting theory successfully accounts for the magnitudes of the thermopower, electrical conductivity, and transverse spin diffusion constant. Moses et al[27] recently presented experimental results which are in excellent quantitative agreement with Kivelson's theory.

The T-dependence of the resistance (R) of trans-$(CH)_x$ is shown in Fig. 12 for P = 219 bars and P = 8.74 Kbars. The variation of R with pressure at T = 300 K is shown in the inset. The measurements were carried out in a teflon cell using Fluorinert as the pressure medium. Independent experiments have demonstrated by means of floatation density measurements that the Fluorinert "wets" the polymer and penetrates into the low density $(CH)_x$ film. Thus the effect of pressure is to compress the fibrils rather than to collapse the low density $(CH)_x$ film.

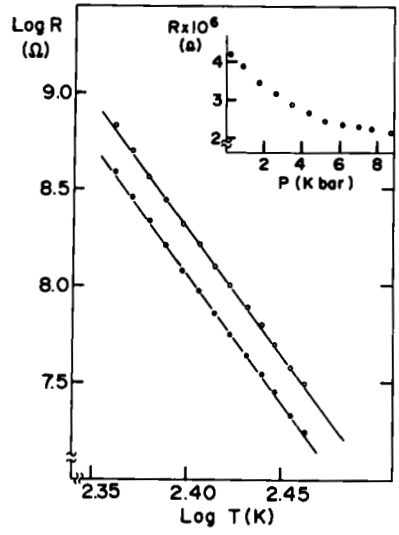

FIGURE 12. Resistance vs Temperature (log-log plot) for trans-$(CH)_x$; o o o P = 219 bars; n = 13.2, o o o P = 8.74 K bars; n = 13.3. The inset shows the pressure dependence at T = 300 K.

Downloaded by [Tomsk State University of Control Systems and Radio] at 03:19 23 February 2013

Downloaded by [Tomsk State University of Control Systems and Radio] at 03:19 23 February 2013

As predicted by Kivelson, the straight line on the log-log plot demonstrates a power law dependence, $\sigma \sim T^n$. The results are typical; experiments carried out with many samples taken from several different preparations of $(CH)_x$ film indicate power law behavior with $n \simeq 13$. The results obtained at different pressures (Fig. 12) indicate that n is independent of P; best fits yield $n = 13.3$ and 13.2 for P = 219 bars and 8.74 Kbar, respectively. Since previous studies demonstrated that the normalized T-dependence is independent of dopant concentration below 0.1 mole %, the power law is characteristic of the dilute doping regime. Indeed, re-plotting earlier data gives consistent behavior.

Within the temperature range of Fig. 12, S is positive and T-independent in agreement with Kivelson's result

$$S = \pm\left|\frac{k_B}{e}\right|\{(n + 2)/2 + \ell n\, y_n/y_{ch}\} \qquad (2)$$

where y_n and y_{ch} are fractional concentrations (i.e. per carbon atom) of neutral and charged solitons, respectively, and the + or - sign designates p-type or n-type. Substitution of n = 13 into eq. 1 with $S \simeq 850$ μV/K yields $\ell n(y_n/y_{ch}) \simeq 2.5$. Since the concentration of neutral solitons in trans-$(CH)_x$ is known from ESR studies,[28] $y_n \simeq 3 \times 10^{-4}$ (1.5×10^{19} cm^{-3} x), we obtain an estimate of the number of charged solitons, i.e. the dopant concentration, in as-grown trans-$(CH)_x$; $y_{ch} \simeq 3 \times 10^{-5}$ (1.5×10^{18} cm^{-3}), in reasonable agreement with depletion measurements on heterojunctions.[8] Thus, the electrical conductivity and thermopower are quantitatively consistent with eq. 2.

Since the magnitude of S is determined in the inter-soliton hopping theory by the electron- phonon coupling, electron-hole symmetry implies that only the sign will change on going from p-type to n-type (eq. 2). Accordingly S was measured for n-doped trans-$(CH)_x$ near the compensation point. Trans-$(CH)_x$ films were electrochemically doped with tetrabutyl ammonium, $(Bu_4N)^+$, to form $[(Bu_4N)_y CH]_x$. Samples were initially doped to $y \simeq 0.03$ and mounted in a sample holder designed for measurements of S vs R. Compensation was achieved by exposure to air over a three day perioed through a slow, controlled leak. Parallel studies have shown that after compensation of n-doped $(CH)_x$ by controlled exposure to air, the infrared and optical properties are essentially indistinguishable from those of as-grown films. During the measurements, the resistance increased from $10^2\Omega$ with S = 43.5 μV/K to $10^8\Omega$ ($\sigma \simeq 5 \times 10^{-6}$ Ω^{-1}-cm^{-1}) with S = -850 ± 130 μV/K near the compensation point. Thus, the universal behavior predicted by eq. 2 is indeed observed in n-type and p-type trans-

$(CH)_x$ at dilute doping levels.

The complete expression for the hopping conductivity is,[26]

$$\sigma(T) = A\left(\frac{e^2}{h}\right)\left(\frac{h\gamma(T)}{k_B T}\right)\frac{y_n \xi}{R_o^2}\frac{y_n y_{ch}}{(y_n + y_{ch})^2} e^{-2BR_o/\xi} \qquad (3)$$

where $A = 0.45$, $B = 1.39$, $\xi = [\xi_{\|}\ \xi^2]^{1/3}$ and $R_o = [(\frac{4\pi}{3})c_i]^{-1/3}$ separation between impurities with concentration c_i (assuming complete charge transfer $c_i = Ny_{ch}$ where N is the density of carbon atoms). Since $\xi_{\|} \simeq 7a \simeq 10\text{Å}$ and $\xi \sim 3\text{Å}$, the effective localization length is $\xi \sim 5\text{Å}$. The rate, $\gamma(T)$, has been estimated by Kivelson as $\hbar\gamma(T) \simeq 500(T/300)^{n+1}$ eV. Using this eq. 3 with $y \simeq 3 \times 10^{-4}$ and $y_{ch} \simeq 3 \times 10^{-5}$, one obtains $R_o/\xi \simeq 6$. The implied value of $R_o \simeq 30$ Å corresponds to $c_i \simeq 8 \times 10^{18}$ cm^{-1}, in satisfactory agreement with experiment.

Examination of eq. 3 shows that the dominant effect of pressure is to change the magnitude through the exponential dependence on (R_o/ξ). Thus, $d(\ell n\sigma)/dP \sim -B(R/\xi)$ where is the compressibility. From Fig. 12, $d(\ell n\sigma)/dP \simeq 7 \times 10^{-11}$ cm^2/dyne, thus giving $\kappa \simeq 8 \times 10^{-12} cm^2$/dyne for <u>trans</u>-$(CH)_x$. For comparison, the measured value of κ for <u>cis</u>-rich polyacetylene is 4×10^{-12} cm^2/dyne.[29]

The T-dependence of R for <u>trans</u>-$(CH)_x$ is shown over a wider range in Fig. 13. The data extend from 140 K to 325 K and span about six decades of resistance. The dashed straight line through the data represents power law behavior. Deviations from the simple power law are small, but clearly evident. Also shown for comparison is a least square fit of the data to the form appropriate to variable range hopping, $\exp-(T_o/T)^{1/4}$, with $T_o = 2.5 \times 10^9$ K. Results from different samples give slopes and magnitudes in excellent agreement, but show slight variations in curvature on the log-log plot.

The good fit to the $\exp-(T_o/T)^{1/4}$ dependence suggests the possibility of variable range hopping (VRH) between localized states in the energy gap.[30] The conductivity in the VRH model is given by $\sigma = \sigma_o \exp[-(T_o/T)^{1/4}]$ where $T_o = 16/[\xi^3 N(E_F)k_B]$ and $\sigma_o = 16(e^2/h\xi)(h\omega_{ph}/k_B T_o)(R_o/\xi)^2$, $N(E_F)$ is the density of localized states at the Fermi energy, k_B is the Boltzmann constant, and ω_{ph} is the phonon assisted attempt frequency. With increasing pressure the density of localized states in the gap increases, $\delta N(E_F)/N(E_F) \simeq -[\delta E_g/E_g + \delta V/V]$, so that

$$\sigma = \sigma_o \exp\{-T_o/T)^{1/4}[1-\tfrac{1}{4}(\varepsilon + \kappa)P]\} \qquad (4)$$

Downloaded by [Tomsk State University of Control Systems and Radio] at 03:19 23 February 2013

Downloaded by [Tomsk State University of Control Systems and Radio] at 03:19 23 February 2013

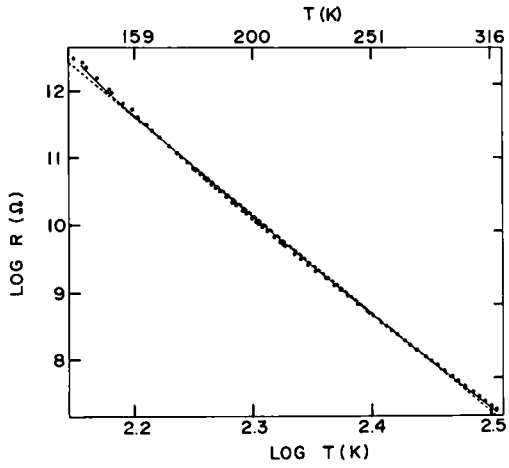

FIGURE 13. Resistance vs Temperature (log-log plot) over an extended temperature range. The dashed straight line represents power law behavior; the solid curve represents a best fit to the $\exp[-(T_0/T)^{1/4}]$ dependence.

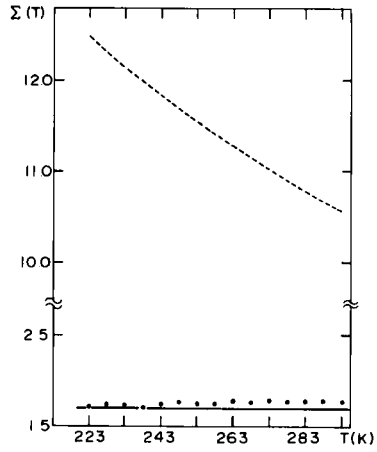

FIGURE 14. Comparison of $\Sigma(T) \equiv \sigma(T,8.74\text{Khar})/\sigma(T,0)$ to the experimental results (black dots); ——— Kivelson theory, ----- variable range hopping.

Downloaded by [Tomsk State University of Control Systems and Radio] at 03:19 23 February 2013

where $\delta E_g/E_g \equiv \varepsilon P$ is the fractional change in energy gap with pressure, ($^{g}\simeq$ 10% at 8.74 kbar). Thus, for VRH, $\sigma(T,P)$ does not separate into T and P independent factors. The ratio $\sigma(8.74 \text{ kbar})/\sigma(o) \equiv \Sigma(T)$ is plotted in Figure 14 and compared with the data as obtained from Fig. 12. The constant experimental value is in clear disagreement with VRH. On the other hand, the factorization of $\sigma(T,P)$ in the Kivelson theory predicts the constant ratio. Furthermore, the value for $T_o = 2.5 \times 10^9$ obtained from the fit in Fig. 13 is two orders of magnitude larger than that found typically in amorphous semiconductors. As a result, assuming $\omega_{ph} \sim 10^{13}$ and $\xi \simeq 10\text{Å}$, the VRH conductivity is estimated to be more than fifteen orders of magnitude below the experimental value! We conclude that the experimental results rule out variable range hopping as the mechanism for transport.

Deviations from the power law dependence can be expected within Kivelson's theory, since the precise temperature dependence arises from the detailed form of the electron-phonon coupling function, g(E), which determines the hopping rate. As an initial approximation, Kivelson chose a simple fitting function to model g(E). More accurate evaluation of the T-dependence requires detailed numerical calculations, which are not currently available. Moreover, eq. 3 assumes freely diffusing neutral solitons, whereas resonance studies have shown that trapping and slowing down of the diffusing neutral kinks becomes important at low temperatures. This has the effect of reducing the number of available neutral solitons (y_n in eq. 3), leading to a steeper T-dependence. Finally, given the dependence of R upon P, thermal contraction may cause an additional temperature dependence through the exponential dependence of $\sigma(T)$ on R_o. Correction for these two effects would lead to more nearly straight line behavior on Fig. 13.

IV. SUMMARY

The soliton concept as applied to polyacetylene has been reviewed and compared with experimental results. The recent observation of the dimerization distortion by Fincher et al has verified the existence of the broken symmetry ground state fundamental to the existence of solitons in trans-$(CH)_x$. The magnetic susceptibility results obtained from an IBM-PENN joint experiment are consistent with the soliton doping mechanism. These recent data again demonstrate that it is possible to prepare highly conducting samples ($\sigma \sim 10^2 \Omega^{-1}\text{cm}^{-1}$) for Y ~ 3-4% with extremely low susceptibility. The steplike

increase near Y = 7% makes the measured values particularly sensitive to dopant uniformity. Hence any residual χ_p in this intermediate regime (Y < 7%) may be the result of nonuniform doping. We conclude that for dilute and intermediate doping (Y < 7%) the decrease of the Curie-Law contribution with no Pauli susceptibility has been demonstrated. The charge carriers are spinless consistent with the soliton doping mechanism.

The electrical transport results can also be understood in the context of the soliton theory. Kivelson's theory of transport by inter-soliton hopping accounts for the magnitude, anisotropy, and pressure dependence of the electrical conductivity, for the magnitude and sign of the temperature independent thermopower, and for the transverse spin diffusion observed in magnetic resonance experiments. Thus, using the soliton theory as a basis, a quantitative understanding of electrical transport in lightly doped trans-$(CH)_x$ has been demonstrated.

ACKNOWLEDGEMENT

The authors are grateful for input from a large number of people. In particular we thank C.R. Fincher, Jr., S. Etemad, D. Moses, Y.-W. Park, J. Flood, S. Ikehata, T.C. Clarke, M. Druy, T. Woerner and L. Lauchlan for important contributions. The structural studies were supported by the NSF-MRL (DMR 7923647), the magnetic studies were supported by the NSF (DMR80-09822) and the transport work was supported by DARPA/ONR on a grant monitored by ONR.

REFERENCES

1. J.T. Devreese and V.E. van Doren, Highly Conducting One-Dimensional Solids (Plenum Press, N.Y. 1979).
2. J.C. Scott, H.J. Pedersen and K. Bechgaard, Phys. Rev. Lett. 45, 2125 (1980).
3. K. Bechgaard, C.S. Jacobsen, K. Mortensen, H.J. Pedersen, and N. Thorup, Solid St. Commun. 33, 1119 (1980); D. Jerome, A. Mazaud, M. Ribault, and K. Bechgaard, J. Phys. (Paris) Lett. 41, L95 (1980).
4. Y.W. Park, A.J. Heeger, M.A. Druy and A.G. MacDiarmid, J. Chem. Phys. 73, 946 (1980).
5. C.R. Fincher Jr., M. Ozaki, M. Taraka, D. Peebles, L. Lauchlan, A.J. Heeger and A.G. MacDiarmid, Phys. Rev. B20, 1589 (1979).

Downloaded by [Tomsk State University of Control Systems and Radio] at 03:19 23 February 2013

6. P.J. Nigrey, A.G. MacDiarmid and A.J. Heeger, J.C.S. Chem. Comm. 594 (1979).
7. P.J. Nigrey, D. MacInnes Jr.,D.P. Nairns, A.G. MacDiarmid and A.J. Heeger, J. Electrochem. Soc. 128, 1651 (1981); D. MacInnes Jr., M.A. Druy, P.J. Nigrey, D.P. Nairns, A.G. MacDiarmid, and A.J. Heeger, J.C.S. Chem. Comm. 317 (1981).
8. M. Ozaki, D. Peebles, B.R. Weinberger, A.J. Heeger, and A.G. MacDiarmid, J. Appl. Phys. 51, 4252 (1980).
9. B.R. Weinberger, S.C. Gaw and Z. Kiss, Appl. Phys. Lett. 38, 555 (1981).
10. S.N. Chen, A.J. Heeger, Z. Kiss, A.G. MacDiarmid, S.C. Gaw and D.L. Peebles, Appl. Phys. Lett. 36, 96 (1980).
11. T.-C. Chung, A. Feldblum, A.J. Heeger, and A.G. MacDiarmid, J. Chem. Phys. 74, 5504 (1981).
12. W.P. Su, J.R. Schrieffer, and A.J. Heeger, Phys. Rev. Lett. 42, 1698 (1978); Phys. Rev. B22, 2099 (1980).
13. M.J. Rice, Phys. Lett. 71A, 152 (1979).
14. H. Takayame, Y.R. Lin-Liu and K. Maki, Phys. Rev. B21, 2388 (1980).
15. S. Brazonskii, JETP Lett. 28, 656 (1978); JETP 78, 677 (1980); S. Brazonskii and N. Kirova Pis'mu Zh Eks. Teor. Fiz. 33, 8 (1981).
16. C.R. Fincher Jr., C.-E. Chen, A.J. Heeger, A.G. MacDiarmid, and J. Hastings (to be published).
17. R.H. Baughman, S.L. Hsu, L.R. Anderson, G.P. Pez and A.J. Signorelli, Molecular Metals Ed. by W. Hatfield (NATO Conf. Sever. Plenum Press, New York + London 1979).
18. E.J. Mele and M.J. Rice, Sol. State Commun. 34, 339 (1980); Phys. Rev. Lett. 45, 926 (1980); S. Etemad, A. Pron, A.J. Heeger, A.G. Mac Diarmid, E.J. Mele and M.J. Rice, Phys. Rev. B23, 5137 (1981).
19. S. Ikehata, J. Kaufer, T. Woerner, A. Pron, M.A. Druy, A. Sinak, A.J. Heeger and A.G. MacDiarmid, Phys. Rev. Lett. 45, 1123 (1980).
20. B.R. Weinberger, J. Kaufer, A. Pron, and A.J. Heeger and A.G. MacDiarmid, Phys. Rev. B20, 223 (1979).
21. N. Suzuki, M. Ozaki, S. Etemad, A.J. Heeger, and A.G. MacDiarmid, Phys. Rev. Lett. 45, 1209 (1980); Erratum Phys. Rev. Lett. 45, 1983 (1980).
22. L. Lauchlan, S. Etemad, T.-C. Chung, A.J. Heeger and A.G. MacDiarmid, Phys. Rev. B (in press).
23. S. Etemad, L. Lauchlan, T.-C. Chung, A.J. Heeger and A.G. MacDiarmid, (this volume).
24. Y. Tomkiewicz, T.D. Schultz, H.B. Brom, T.C. Clarke, and G.B. Street, Phys. Rev. Lett. 43, 1532 (1979).
25. A.J. Epstein, H. Rommelmann, M.A. Druy, A.J. Heeger and

Downloaded by [Tomsk State University of Control Systems and Radio] at 03:19 23 February 2013

A.G. MacDiarmid, Sol. State Commun. 38, 683 (1981).
26. S. Kivelson, Phys. Rev. Lett. 46, 1344 (1981).
27. D. Moses, J. Chen, A. Denenstein, M. Kaveh, T.-C. Chung, A.J. Heeger and A.G. MacDiarmid, Sol. St. Commun. (in press).
28. I.B. Goldberg, H.R. Crowe, P.R. Newman, A.J. Heeger, and A.G. MacDiarmid, J. Chem. Phys. 70, 1132 (1979).
29. J.P. Ferraris, A.W. Webb, D.C. Weber, W.B. Fox, E.R. Carpenter and P. Briant, Sol. St. Commun. 35, 15 (1980).
30. N.F. Mott, Phil. Mag. 19, 835 (1969); N.F. Mott, Festkorperprobleme 9, 22 (1969); V. Ambergaokar, B.I. Halperin and J.S. Langer, Phys. Rev. B4, 2612 (1971).

Downloaded by [Tomsk State University of Control Systems and Radio] at 03:19 23 February 2013